Fault Seal Prediction and Uncertainty Estimation of a Water Wet Fault*

Tan Chun Hock[1] and Lothar Schulte[2]

Search and Discovery Article #41029 (2012)*
Posted October 8, 2012

*Adapted from extended abstract prepared in conjunction with poster presentation at AAPG International Convention and Exhibition, Singapore, 16-19 September 2012, AAPG©2012

[1]Talisman Energy, Kuala Lumpur, Malaysia (chtan@talisman-energy.com)
[2]Schlumberger Information Solution, Kuala Lumpur, Malaysia

Abstract

Recent advances in computing power have led to vast improvement on static modeling for both fault modeling and fault seal prediction. Nevertheless, there are still many uncertainty factors that are being built into the seal models and need to be addressed in order to come up with a reliable risking. This paper is dealing with a major water wet fault of a clastic oil reservoir. Consequently, its possible sealing is based on capillary entry pressure. The first part of the paper discusses the estimation of the shale/clay content of the fault. Based on the upscaled well data the shale distribution is modeled using multiple stochastic realization as well as different interpolation algorithm. This approach tries addressing fundamental issues of juxtaposition uncertainty. The shale/clay contents of the fault are estimated based on different algorithm (e.g. Vshale cutoff, Shale Gauge Ratio, Shale Smear Factor etc). The impact of each approach is assessed and reviewed. The results are compared to the simplistic approach of triangulating the Vshale/Vclay of the wells to the fault.

The second part of the paper discusses the estimation of the permeability and the capillary entry pressure using different published empirical algorithm. Again, emphasis is laid on the attempt to estimate the uncertainty range of the properties. The final result is presented by three scenarios representing the low, base and high case. Based on the limited pressure data the pressure difference across the fault resulting from the oil buoyancy is estimated and the sealing likelihood of the fault evaluated.

Introduction

Several deltaic settings including NW Borneo show a high sand shale ratio on the topset can be deemed to high risk in faulted areas. Although many shallow discoveries were made on highly faulted topsets our knowledge on their fault seal capacity has not advanced a lot. Many exploration and development wells drilled in these regions are still suffering from lateral seal breaches.

This paper presents a study of a normal fault zone in a high net to gross sedimentation environment at a depth of less than 1,000 m. The aim of the study is to improve the understanding of fault seal risk as this has been identified as the biggest problem currently present in the NW Borneo reservoirs. This paper however is not the answer of whether the fault is sealing or not but rather it proposes common practices to evaluate the likelihood of the leaking areas.

The data used in this study is from a small discovery field in NW Borneo. In term of stratigraphy, the sediments belong to the Upper Miocene. They consist of stacked deltaic cycles forming sand-shale sequences (55% sand and 45% shale). The datasets consists of a normal fault and four closely spaced wells, two of them on each side of the fault. The set of logs includes Gamma Gay, VShale (VSH), Permeability, Sand Flag and check-shots. Detailed interpreted 3D seismic data was input to the structural model. For the model, a grid spacing of 100x100 m and a vertical resolution of 10 m was used. The VShale, Sand Flag facies and the Permeability log of the four wells were sampled into the model and used for stochastic property modeling.

'Classic' Tools for Fault Seal Analysis

The well triangle diagram delivers an estimation of the Shale Gauge Ratio (SGR) as a function of the fault throw. The SGR is derived from the VSH log. The diagram is a powerful tool to identify depth ranges of potential low SGR. Figure 1 shows the triangle diagram for one of the four wells of the study. Note the dependence of the SGR value with the fault throw!

The Allen diagram can identify areas of potential leakage zones on the fault plane. A powerful modification of the Allen diagram is the juxtaposition display of the facies along the fault. This approach requests a facies model that in our case results from the stochastic indicator simulation based on the upscaled Sand Flag facies logs of the four wells. The facies are closely linked to the VSH: low VSH values indicate sand, high VSH defines shale facies. The variogram model that is needed for stochastic facies simulation was derived from the VSH logs of 14 wells in the vicinity of the study area. These logs deliver a smoother sample variogram than the facies variogram and therefore allow deriving a reliable variogram range. Figure 2 shows the fault with the facies juxtaposition based on a

stochastically simulated facies model. The yellow spots on the fault show the sand – sand juxtapositions that could represent potential leakage zones.

A more accurate way to estimate the leakage potential of the fault is the derivation of the Shale-Gauge Ratio (SGR) along the fault plane (Yielding et al. 1997). The SGR calculation needs a VSH model derived from the upscaled VSH logs of the four wells. This shale model is based on Gauss simulation and conditioned to the facies model that was used for the juxtaposition discussed above.

Figure 3 shows the SGR distribution based on this shale model. Yellow colors indicate low SGR, green and blue colors a high SGR. As a 'rule of thumb' fault areas with an SGR above 30% are 'probably' sealing. This example shows that the juxtaposition diagram of the facies are possibly overestimating the leakage potential of the fault. Apparently, the SGR reduces the areas of possible fault leakage considerably compared to the juxtaposition approach.

Analysis of SGR Uncertainty

In the following, it is assumed that three key parameters are influencing the SGR distribution: the facies model, the VSH model and the fault throw. The depositional environment of the study area justifies building the facies model using sequential indicator simulation. This also means that several equivalent facies models can be calculated, each one having the same geostatistical properties. Consequently, each facies model delivers a different juxtaposition pattern along the fault and a different SGR distribution. Figure 4 shows an example of the SGR distribution for four different facies models. Obviously, an accurate facies model is needed in order to get a reliable SGR distribution and a reliable estimation of the leakage potential of the fault. However, in general due to lack of data the facies model remains highly uncertain.

Therefore, an attempt was made to calculate a fault property showing the probability of encountering a SGR value below 30%. The workflow included the following steps:

- Stochastically simulation of many (100) facies models.
- Simulation of the same number of VSH model conditioned to the facies models.
- Calculation of the SGR for each VSH model.
- Assign a value of '1' to the SGR smaller than 30% and a value of '0' to all other fault cells.
- Stacking of the SGR fault planes.

- Converting of the resultant SGR plane to a probability map thru normalizing its values to 100%.

Figure 5 shows the resultant SGR probability distribution along the fault. Also shown is the average fault throw. Areas of high probability for small SGR values can be observed in the vicinity of the four wells to the left. All wells are less than 1,000 m away from the fault and consequently the facies and VSH distribution in the vicinity of the fault is influenced by the VSH distribution given by the well logs. However, at the right side of the fault another area of potential low SGR values can be seen. This area is outside the variogram range and consequently the low SGR results from the changes of the fault throw. This assumption is backed by the fault throw that is shown in the lower part of the figure: the probability of low SGR is highest in areas with a small fault throw.

Similar to the facies model the VSH modeling is based on Gauss simulation and consequently several equivalent models can be calculated. Each VSH model, which is conditioned to the same facies model, delivers a different SGR distribution. Following the workflow above the probability distribution for SGR smaller than 30% is calculated. Figure 6 shows the facies juxtaposition along the fault and the SGR probability based on 100 simulated VSH models conditioned to the facies model used for the juxtaposition display. Unsurprisingly this distribution deviates considerably from the distribution based on the VSH models conditioned to different facies model simulations.

In order to study the influence of the fault throw on the SGR distribution two structural models were set up with a fault having a throw of 70% and 130% of the throw given by the base case model discussed above. For both models, the workflow described above was applied in order to get the probability distribution of SGR smaller than 30%. Figure 7 shows the probability map for the model with increased fault throw and Figure 8 the probability map for the decreased fault throw model.

Obviously, a reduction of the throw is increasing the areas with low SGR values. On the other hand, an increase of the fault throw will reduce the risk of a fault leakage. It is interesting to compare this result with the triangle diagram of the four wells (see Figure 1). The diagram confirms that with increasing throw the SGR values are increasing and consequently the risk of fault leakage decreasing. But obviously the triangle diagram cannot outline the areas of the fault with increased leakage risk.

Analysis of Capillary Entry Pressure Uncertainty

The fault is assumed to be water wet and consequently the possible leakage is governed by the capillary entry pressure. The workflow that was used for estimating the capillary entry pressure is given in the following:

- Calculate the SGR distribution.
- Convert the SGR to permeability using the VSH-Permeability relationship given by the logs.
- Convert the permeability to the capillary entry pressure using the empirical formula of Sperrevik et al. (2002).
- Conversion of the capillary entry pressure to gas column height.

In order to study the influence of key parameters on the capillary entry pressure a base case scenario was defined and for one parameter at the time its value range estimated and the capillary entry pressure range calculated. This analysis was not done for all SGR values of the fault but only for the P1 value of the SGR model. This approach is reducing considerably the amount of work and is justified by the fact that the low SGR values decide on the leakage or sealing capacity of the fault.

The value range of the key parameters was estimated in the following way:

- Facies distribution: For 100 facies models, the VSH distribution was simulated and the SGR calculated. For each SGR distribution, the P1 value was extracted. The minimum and maximum P1 value was converted to capillary entry pressure using the base parameters.
- VSH stochastic model: 100 VSH models were stochastically simulated and the SGR distribution calculated. From these results, the SGR P1 minimum and maximum was derived and converted to capillary entry pressure.
- Variation in mean VSH: a VSH stochastic model was made using the upscaled data of one well at the time. The derived SGR for each simulation delivered the P1 value range used for the capillary entry pressure calculation.
- Fault throw: two additional structural models were built with a fault throw 30% lower and higher than the fault throw of the base case model. For each model, 100 facies distributions were simulated and the capillary entry pressure range derived as explained above.
- Uncertainty of Permeability (Figure 9): the VSH and the Permeability logs of the four wells in the vicinity of the fault were cross-plotted. The best-fit curve gave the VSH-Permeability relationship for the base case. The envelope around the data points delivered the low case and the high case scenario. Outliers were ignored when estimating the envelope.
- Uncertainty of capillary entry pressure (Pc) (Figure 10): the formula of Sperrevik et al. (2002) was used for the base case scenario. The low case and the high case were defined by the envelope around the data points used by Sperrevik et al. (2002) for their best-fit curve.

The result of the sensitivity analysis is presented in form of a tornado diagram (Figure 11). To better visualize the capillary entry pressure its values were converted to gas column height. Obviously, the determination of the permeability and capillary entry pressure (Pc) from the derived functions delivers the largest uncertainty. This is the consequence of the large scatter of the data around the best-fit curve.

Conclusion

The 'classic' approach for fault seal analysis, triangle diagram, facies juxtaposition and SGR calculation based on the facies and shale models may give misleading results. This problem arises from the uncertainty of the modeled shale, facies and fault throw. The calculation of several SGR using different equivalent facies and VHS models shows the difficulty in defining the location of fault areas that are leaking or sealing. The discussed SGR probability maps try to address this problem.

The estimation of the capillary entry pressure is based on the SGR calculation, which is subject to large uncertainty. However, the 'heavy-hitter' parameters that are most influential on the uncertainty of the capillary entry pressure estimation are the functions used for deriving the permeability and the pressure. Consequently, the derived capillary entry pressure should be used with greatest care.

Acknowledgement

We would like to thank Talisman for providing the data and Talisman and Schlumberger for continuous support of this work.

References

Sperrevik, S., P.A. Gillespie, Q.J. Fisher, T. Halverson, and R. J. Knipe, 2002, Empirical estimation of fault rock properties, *in*: A.G. Koestler, and R. Hunsdale, (eds), Hydrocarbon Seal Quantification: NPF Special Publication 11, Elsevier, Amsterdam, p. 109-125.

Yielding, G., B. Freeman, and D.T. Needham, 1997, Quantitative fault seal prediction: AAPG Bulletin, v. 81/6, p. 897-917.

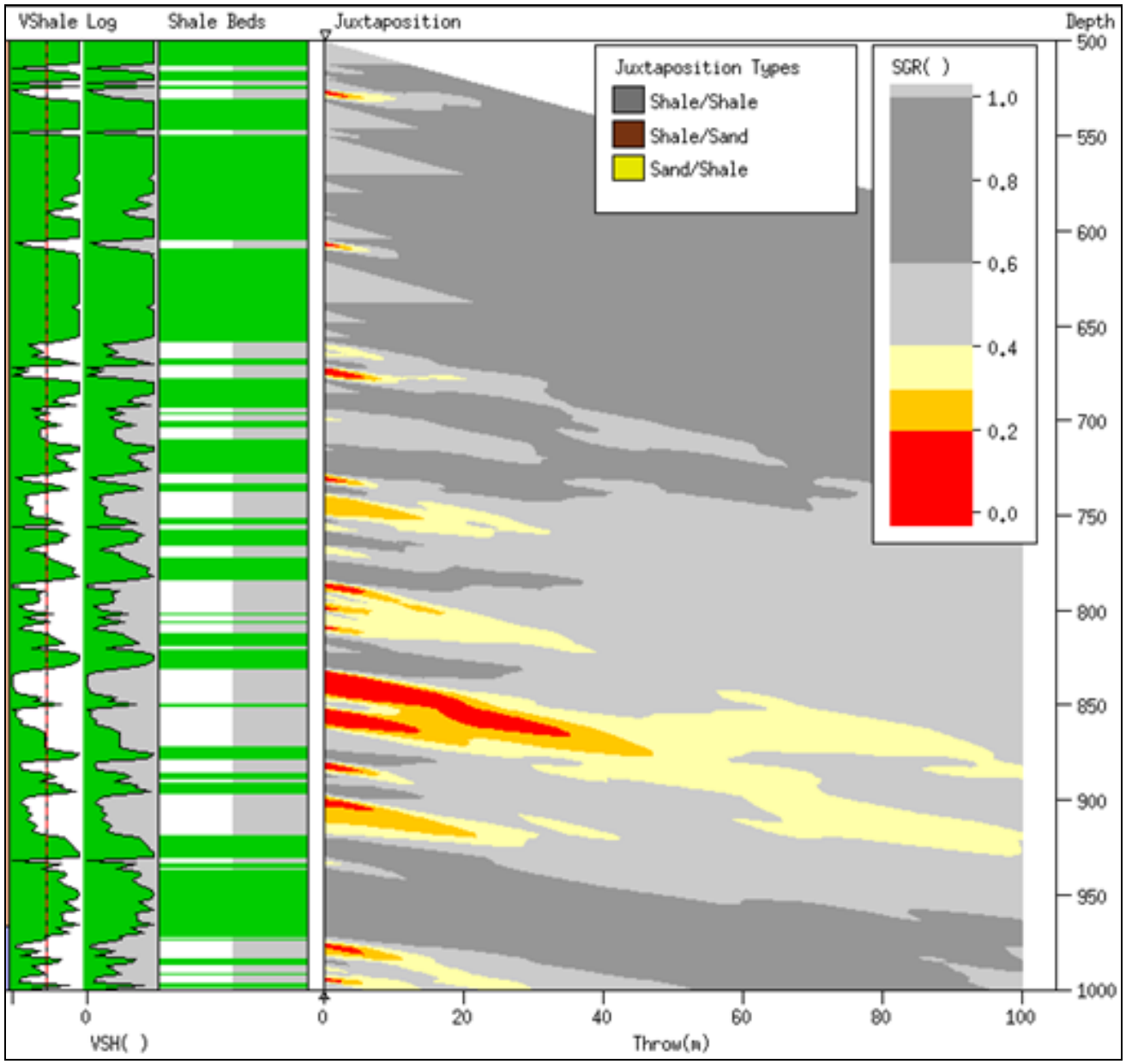

Figure 1. Triangle diagram of one of the study area showing the SGR distribution derived from the VSH log at one well. The distribution is plotted as a function of the throw. Note the relationship between low SGR and throw.

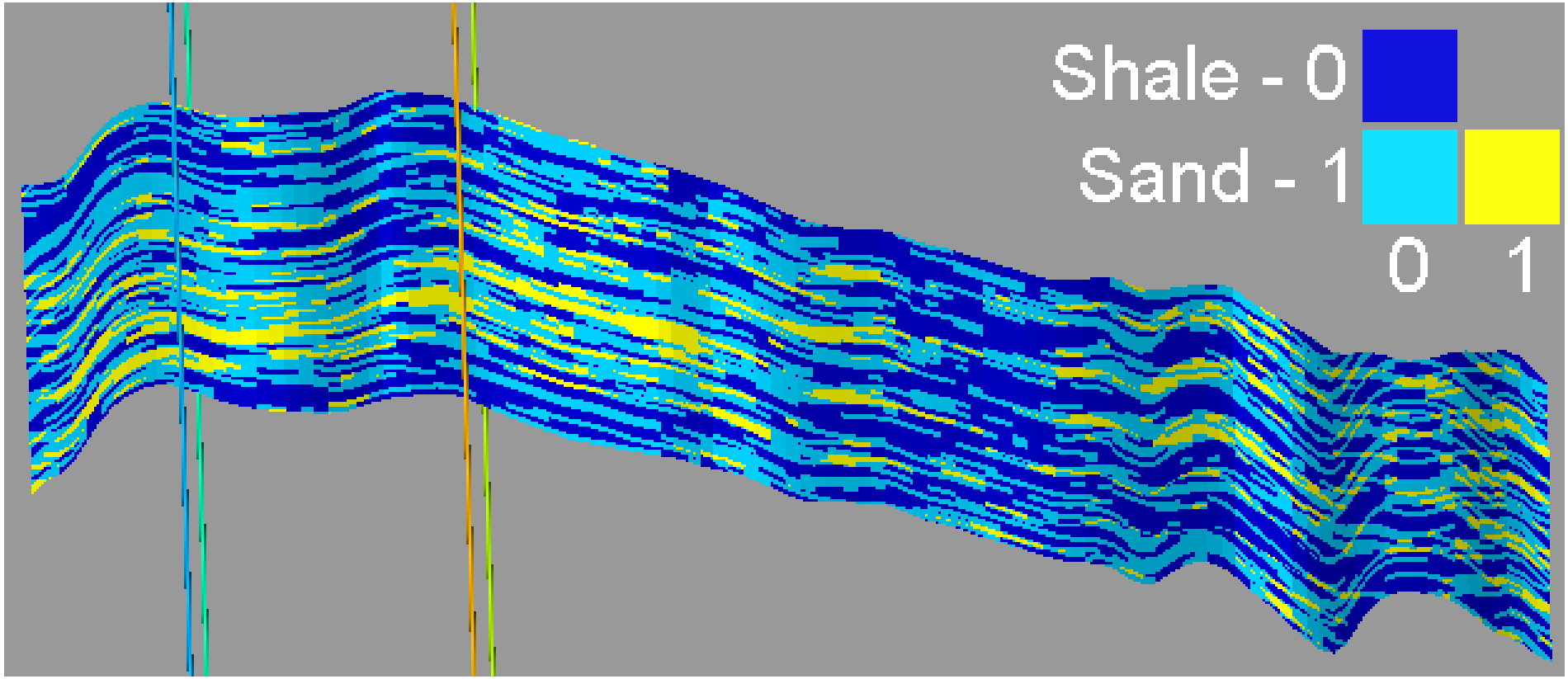

Figure 2. Facies juxtaposition along the fault based on a stochastically simulated facies model.

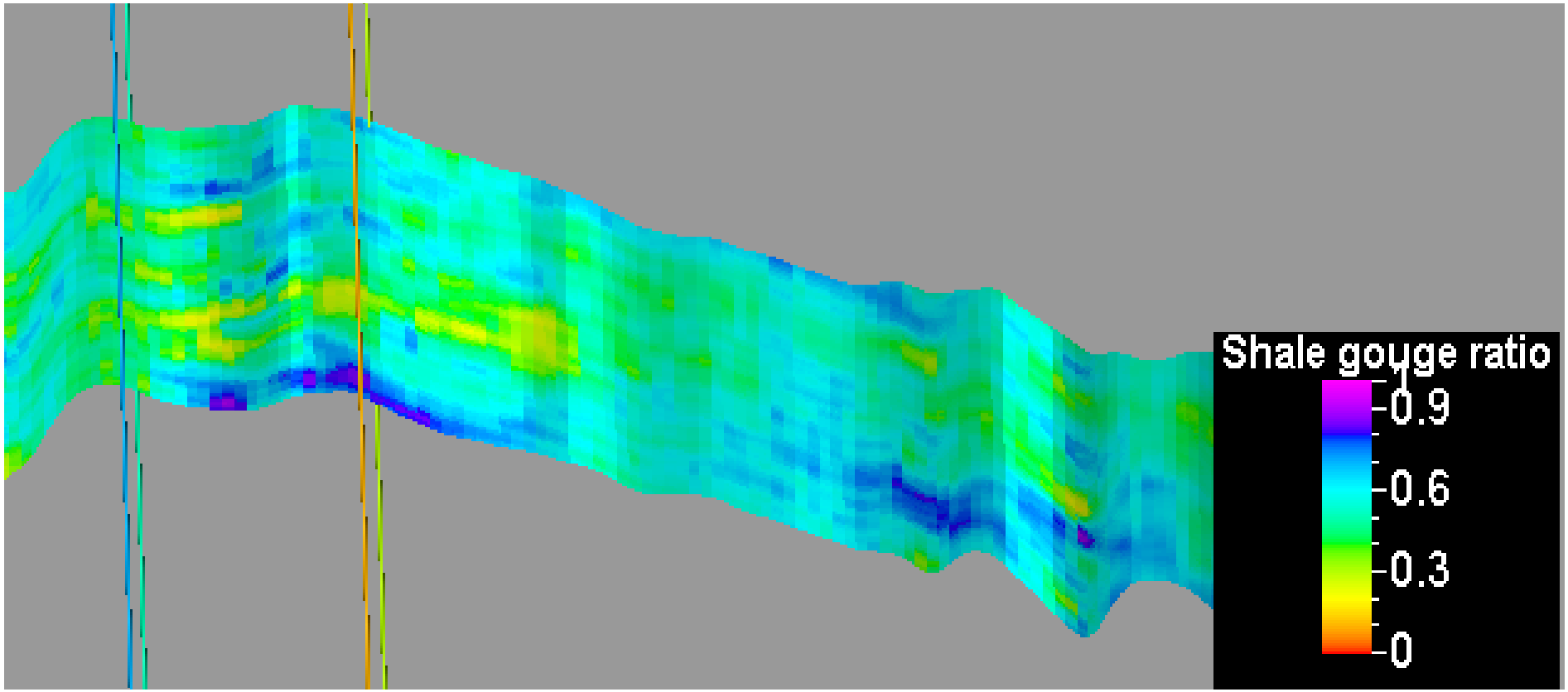

Figure 3. SGR distribution along the fault.

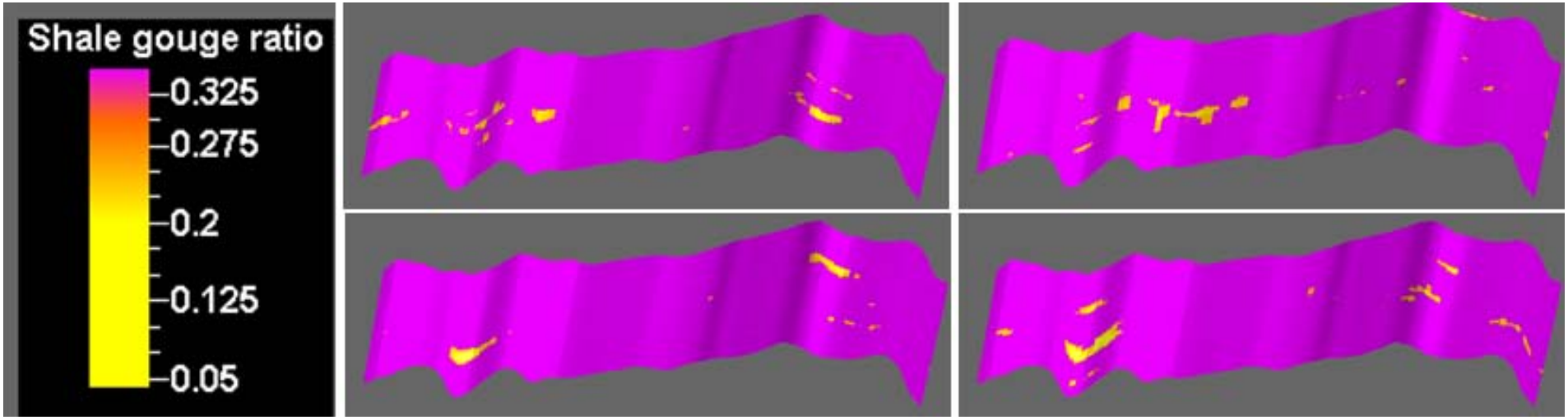

Figure 4. SGR distributions based on different facies simulations. In order to highlight the SGR values below 30% all other SGR values are displayed in one color.

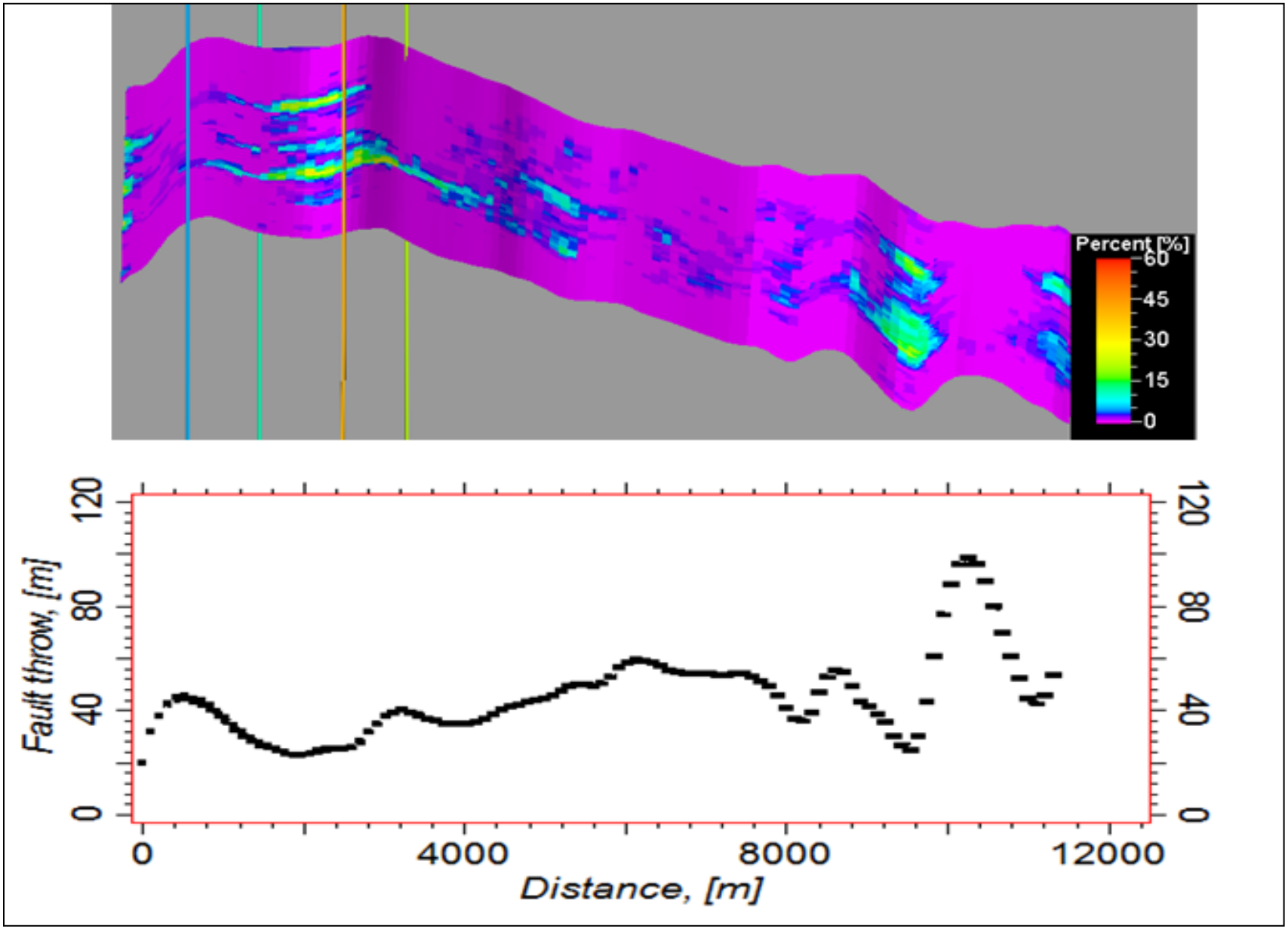

Figure 5. Top: Probability distribution of SGR <30%; Bottom: Average fault throw. Note: high probability of SGR<30% is linked to small fault throws.

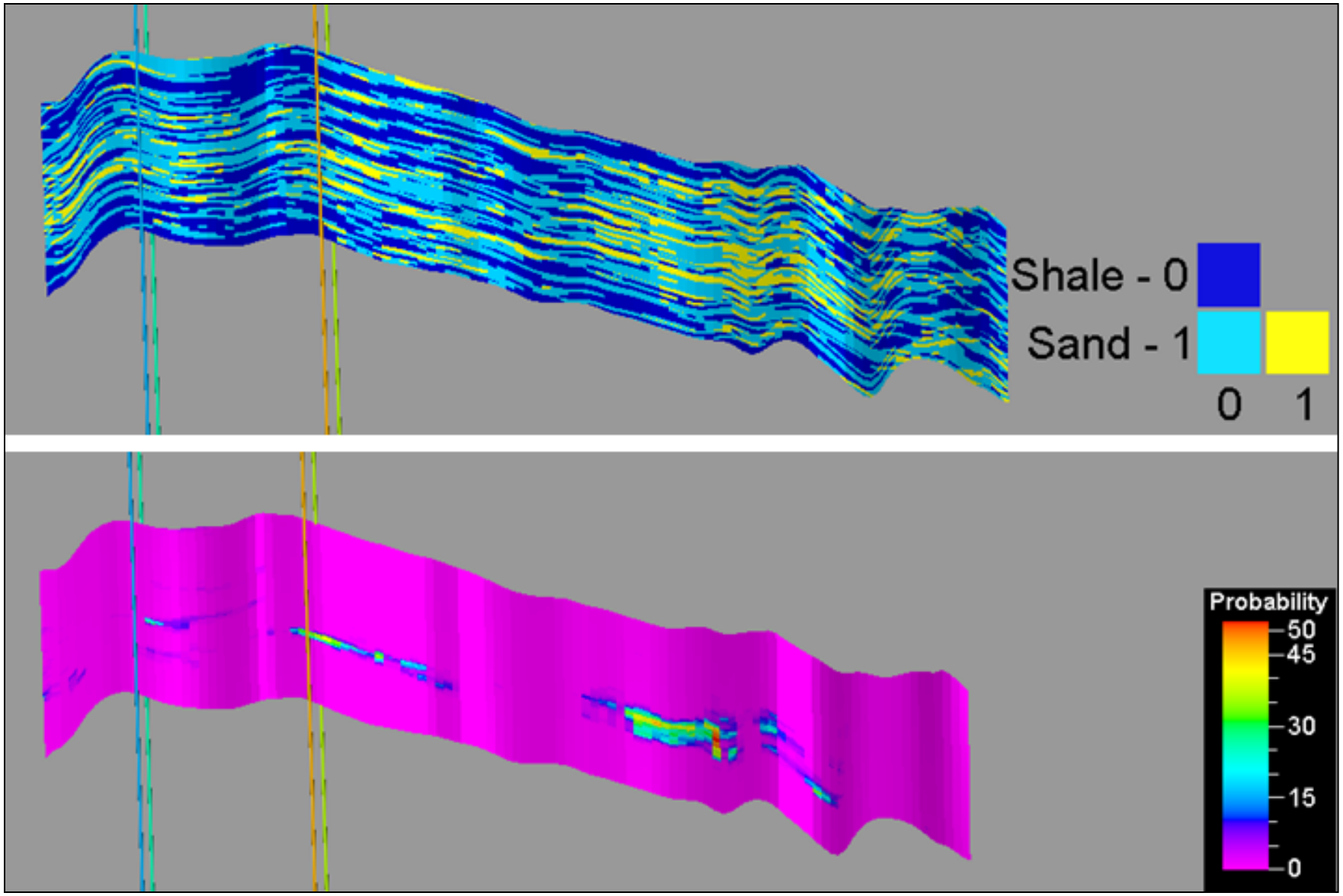

Figure 6. Top: Juxtaposition of facies. The underlying facies model is used for the 100 realizations of the VSH property used for deriving the probability map for SGR<30% shown in the lower figure.

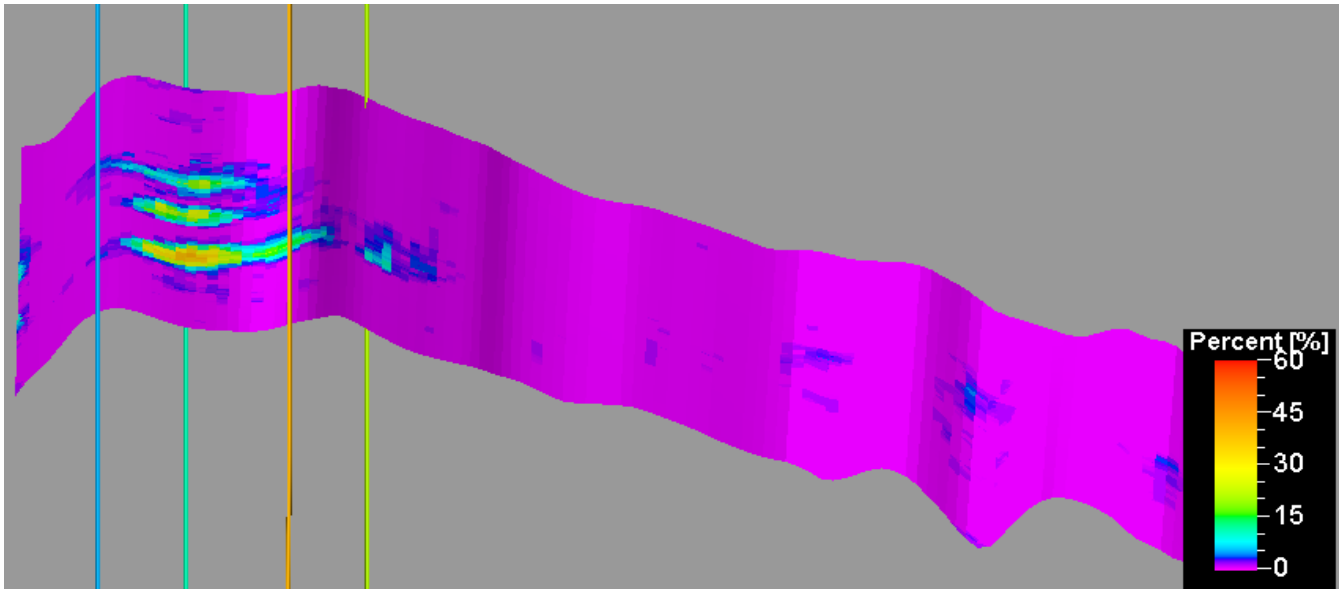

Figure 7. Probability plot for SGR <30 and a fault throw that is 30% higher than the base case fault.

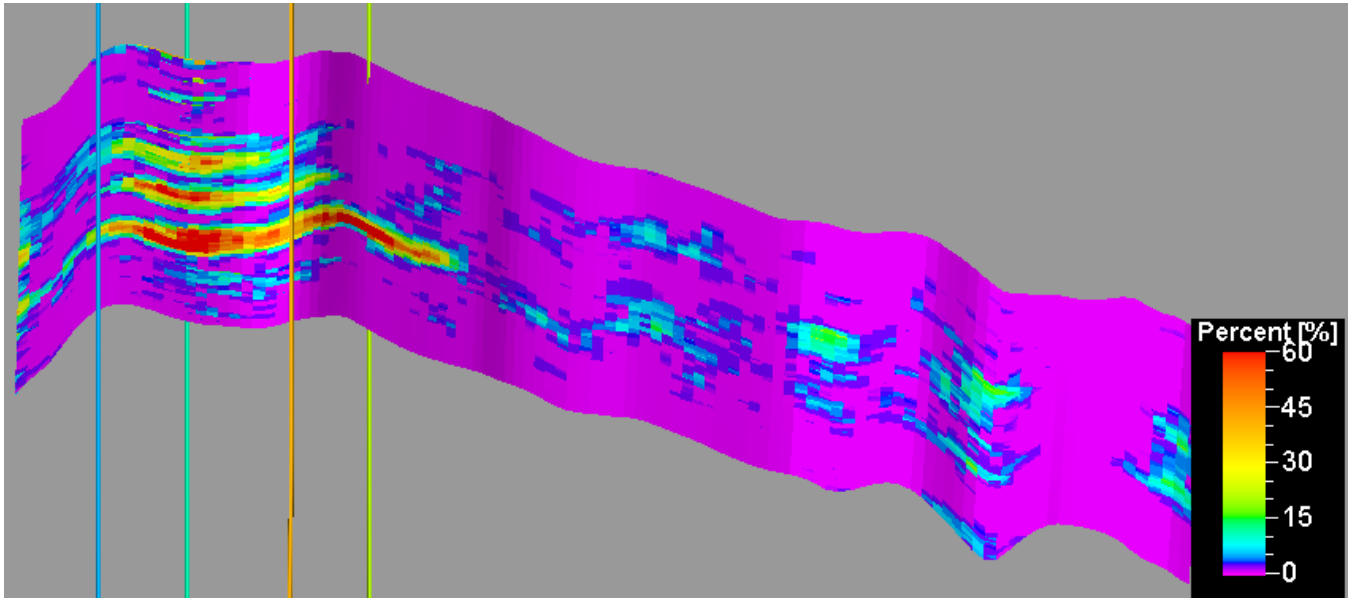

Figure 8. Probability plot for SGR <30 and a fault throw that is 30% smaller than the base case fault.

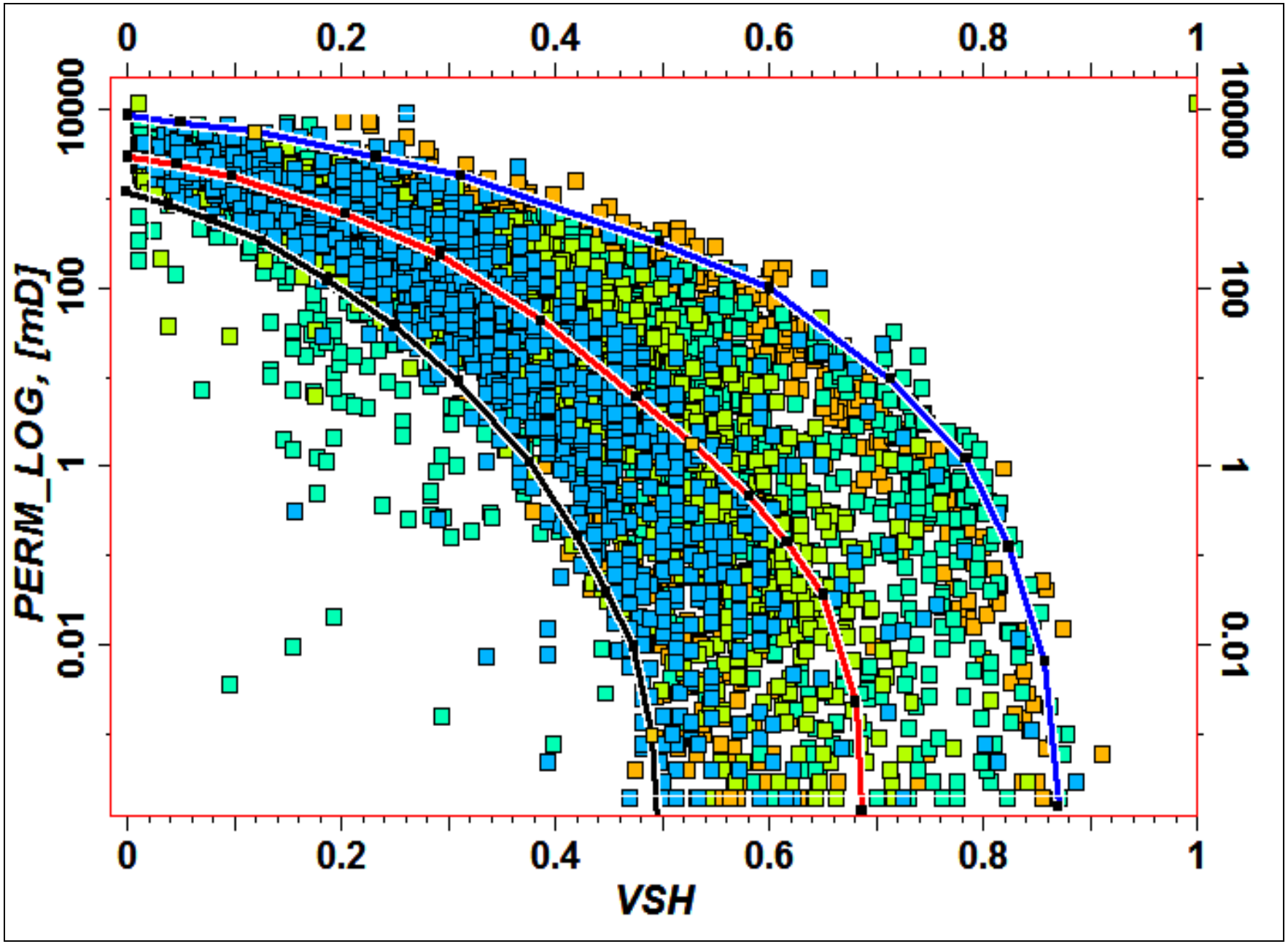

Figure 9. Cross-plot of the VSH log vs. Permeability log for the depth range of the study area. The three lines define the low case, base case and the high case functions used for the permeability calculation.

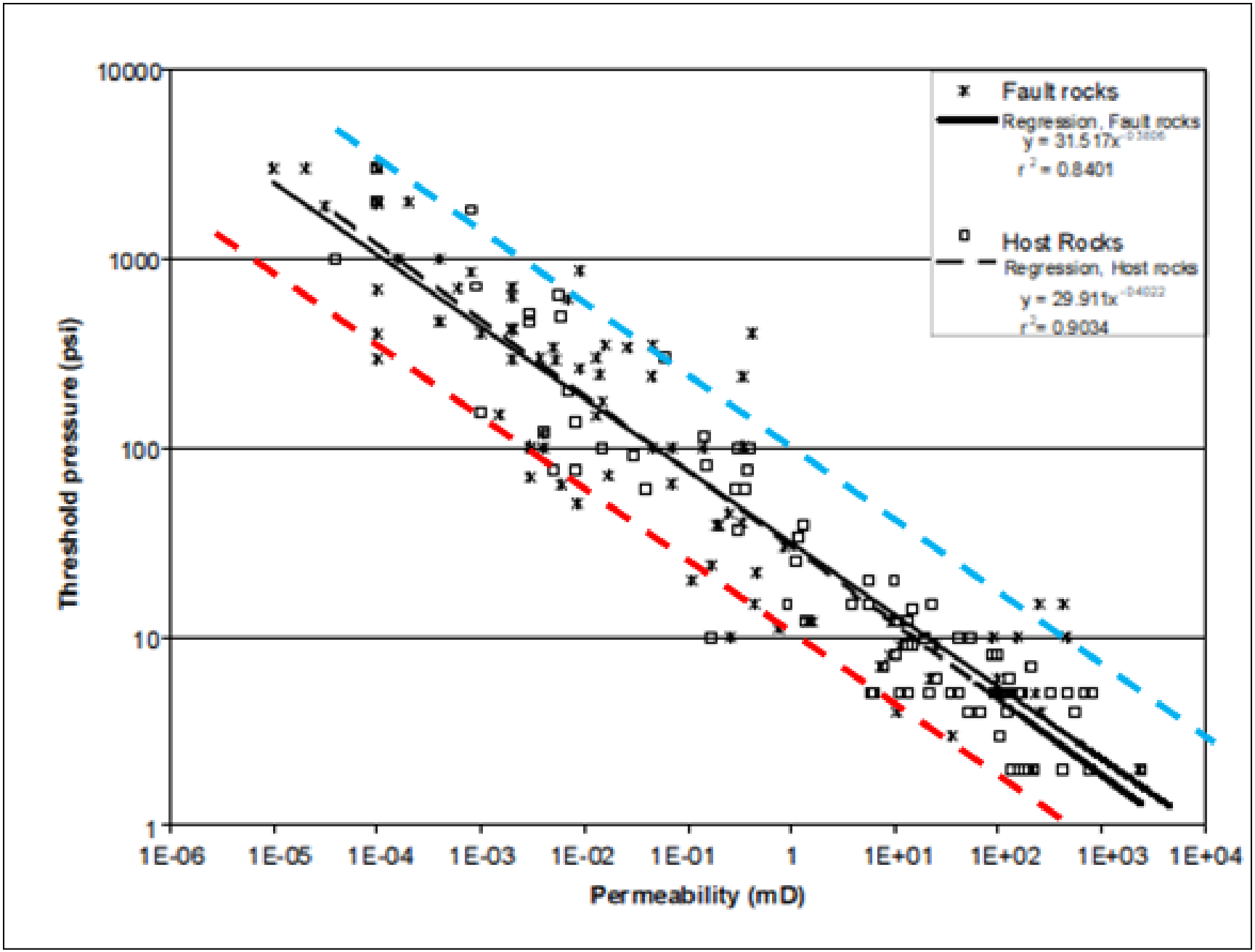

Figure 10. Permeability – Threshold pressure relationship modified from Sperrevik et al. (2002). The red and blue lines were used for the low and high case scenario.

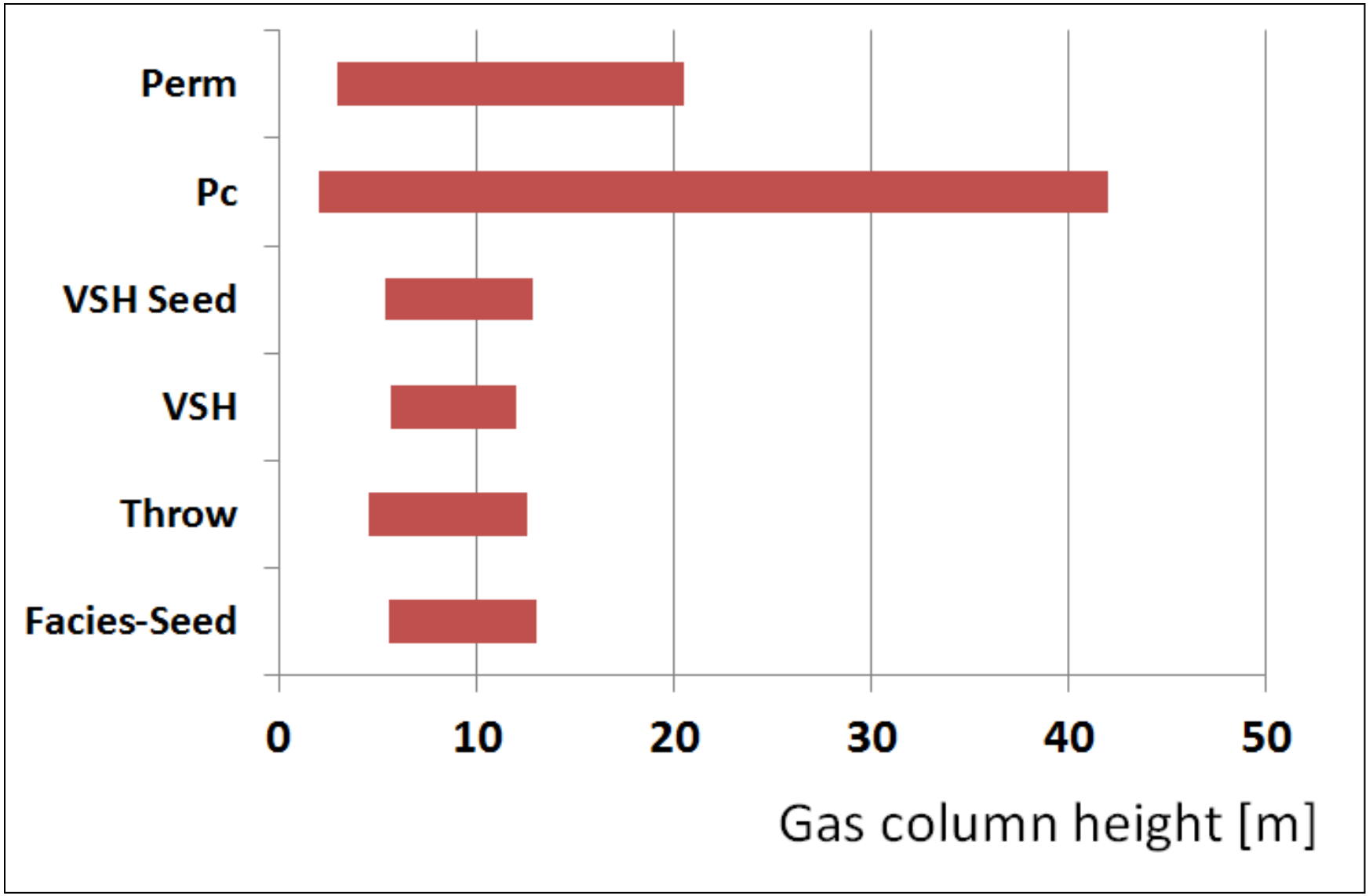

Figure 11. Tornado diagram of the key parameters used for estimating the capillary entry pressure. The pressure data were converted to gas column height.